

STOCHASTIC MODELING OF IMPURITY MOTION AND SCATTERING IN THE MECHANICS OF TURBULENT GAS-DISPERSED FLOWS

K. N. Volkov

UDC 532.529:536.24

Issues associated with the development and realization of stochastic models of the impurity particle motion and scattering in a turbulent flow are considered. The proposed model is used to calculate turbulent flows of a low-concentration gas suspension in channels and jets. We compare the results of the calculations obtained from the viewpoint of different models and the results of numerical simulation with the data in which the influence of turbulent pulsations on the particle motion was ignored.

Introduction. To describe and forecast the properties of gas-disperse systems, the following approaches are usually used: the kinetic, continual, and trajectory ones (Fig. 1). Practical realization of a particular approach is determined, first of all, by the applicability limits and the possibility of predicting various characteristics of the flow.

The kinetic approach finds application in works considering the construction and substantiation of mathematical models of dispersive media. In solving specific problems, kinetic models are used comparatively rarely because of the difficulty of solving the necessary equations. Its application is reasonable in problems with fairly small particles as well as in the cases where corrections associated with impurity concentrations become important. In other situations, the use of the kinetic approach seems to be unjustifiably awkward and complicated.

As applied to the modeling of turbulent flows, kinetic models are suitable for obtaining equations for the moments of fluctuating parameters of the gas and dispersed phases [1].

The continual approach considers the interpenetrating motion of several interacting continua connected with gas and particles. The dispersed phase is represented in the form of a continuous medium with a continuously space-distributed density. The characteristics of the continuum connected with the dispersed phase are interpreted as local mean values of the particle parameters. The behavior of a multispeed continuum is described by the equations of continuous medium mechanics in Euler coordinates. The positive part of the continual approach consists in that, in principle, it is possible to describe the motion of the gas and the dispersed phase from a single point of view. The succession of models permits counting on a fairly universal description of many complex processes.

Modeling of turbulent flows of a gas suspension within the framework of the continual approach requires the solution of two basic questions associated with the determination of the degree of involvement of particles in the pulsation motion of the carrier flow and the description of the reverse effect of impurity on the field turbulence. To resolve these questions, one uses the Prandtl mixing path model and the equations for second one-point moments of fluctuating parameters of the gas and dispersed phases [1, 2]. The use of the equations for second moments permits taking into account, without the heuristic assumptions characteristic of the mixing path, the reverse effect of impurity, as well as the convective and diffusion transfer. The correlation moments connected with the dispersed phase are found either by using the space-time averaging method [2] or on the basis of the probability density function method [1]. For hydrodynamically quick-response particles, the diffusion (only the diffusion impurity transfer is taken into account) or the diffusion-lag (besides the diffusion transfer, the particle migration is taken into account) approximation is used [1]. The application of simplified models leads to large errors near the wall where the particles become hydrodynamically more sluggish.

In the trajectory approach, the equations describing the impurity motion are written in Lagrangian coordinates and are integrated along the trajectories of individual particles in the known (preliminarily calculated) gas-dynamic

D. F. Ustinov Baltic State Technical University (VOENMEKh), 1 1st Krasnoarmeiskaya Str., St. Petersburg, 190005, Russia; email: root@kv7340.spb.edu. Translated from *Inzhenerno-Fizicheskii Zhurnal*, Vol. 77, No. 5, pp. 10–19, September–October, 2004. Original article submitted September 17, 2004.

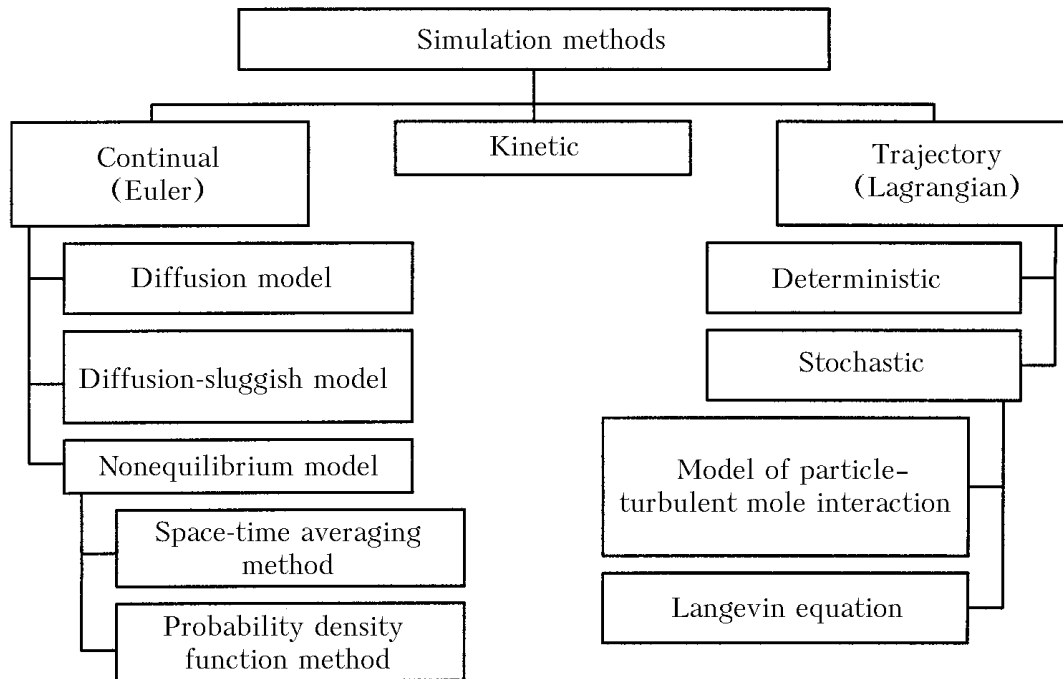


Fig. 1. Approaches to the calculation of turbulent flows of gas suspension.

field. In the calculation mesh cells, information on the dispersed-phase parameters and the particle–gas interaction is accumulated. The reverse effect of the dispersed phase on the gas flow is taken into account on the basis of global iterations [3].

Compared to the continual approach, the trajectory approach requires simple and physically more correct closing assumptions that permit revealing, with a high degree of detailing, the structure of the flow. However, to initiate the impurity motion, a fairly representative ensemble of particles is needed. Moreover, the trajectory approach features difficulties arising in describing a large number of interrelated physicochemical processes, which show up as an inter-phase interaction.

Depending on the model of particle interaction with the carrier medium, in particular, with the pulsation component of the turbulent flow velocity, the deterministic and stochastic variants of the trajectory approach are distinguished [3, 4].

In the deterministic model, the interaction of discrete inclusions with turbulent moles, which holds only for rather sluggish particles, is ignored. The position of the probe particle at the initial instant of time completely determines its further evolution on the only mechanical trajectory. In flows with a large curvature of streamlines, melting and burning of particles (twisted jets, atomizers, mass-supply channels), the model leads to errors in determining the characteristics of the two-phase flow [1, 3, 5].

The stochastic model takes into account the influence of turbulence by introducing a random force into the equation of particle motion. The instantaneous velocity of the turbulent flow is represented as the sum of the averaged and random components: the first component is calculated on the basis of the Reynolds equations and the second one is determined on the basis of the Monte Carlo method.

The interaction of a particle with turbulent moles leads to a chaotic impurity motion, and the particle position at a given instant of time determines only the probability of its stay in the aggregate of states at each subsequent instant of time. The obtaining of a reliable averaged picture of the impurity motion requires calculation of a rather large number of probe particles.

Another possible approach to the modeling of the particle dispersion in a turbulent flow is to use the Langevin equation, whose integration is based on the Markov chain theory [6].

The stochastic models described in the literature are distinguished by physical factors that are taken into account and peculiarities of generating turbulent fluctuations of the carrier flow rate. The present paper considers the fea-

tures of the formulation and realization of different stochastic models of the impurity motion and scattering. Internal and jet flows of a low-concentration gas suspension (the reverse effect of particles is ignored) are calculated and the results obtained on the basis of the deterministic and stochastic models are compared. Comparison of the results of calculations from the point of view of different models makes it possible to answer the question to what extent is the application of a particular approach justified and how significant is the influence of the carrier, flow pulsations on the impurity motion and scattering.

Modeling of the Carrier Phase. The realization of the stochastic model of impurity motion in the turbulent flow requires calculation of both the medium field and the pulsation field of the carrier gas. To calculate the characteristics of the carrier phase, various approaches differing from one another in the degree of detailing of the flow pattern and the complexity of realization are used.

1. Semiempirical relations obtained on the basis of the experimental data processing or the results of direct numerical simulation. Their disadvantage is associated with the narrow limits of applicability, since they hold only for a concrete type of flow and that range of parameters for which measurements were made. Such relations are widely used to calculate internal and jet flows [7], in particular, to model the impurity dispersion in nonisothermal gas and plasma jets [8, 9].

2. Monoharmonic models in which the pulsation component of the carrier-phase velocity is given in the form

$$v'_i = v_{i\max} \sin \omega t .$$

The amplitude and frequency are assumed to be known. Such models are widely used to calculate the particle motion in technological units, where induced pulsations are imposed on the gas velocity, as well as particle vibrations in a sound field [2].

3. Equations of the two-parametric turbulence model, which leads to the necessity of reconstructing the carrier-phase fluctuation field by calculated average parameters (in averaging, information on the instantaneous structure of the flow is lost). Velocity fluctuations are usually calculated in the local-isotropic and local-homogeneous approximation $v'_i = (2k/3)^{0.5}$. In the three-dimensional case, the probability density is given by the relation

$$p(v') = \left(\frac{3}{4\pi k}\right)^{1/2} \exp\left(-\frac{v'^2}{4k/3}\right).$$

Modeling of fluctuating parameters of the turbulent flow by the normal probability distribution is justified only in some particular situations, e.g., at turbulent diffusion of a zero-lag impurity from a point source in a homogeneous isotropic turbulence [4]. However, in more complicated problems, too, the use of the normal probability distribution yields satisfactory results [5, 6, 8, 9].

The assumption of turbulence isotropy leads to an overestimation of fluctuations of the velocity component normal to the wall [10, 11]. To take into account the flow anisotropy, damping functions are introduced. They are constructed on the basis of experimental data or results of direct numerical simulation [12]. As for the semiempirical relations, the range of applicability of a damping functions is limited by the range of parameters for which measurements and calculations were made.

4. Transfer equations of Reynolds stresses. Fluctuations of the carrier-phase velocity are found from the normal components of the Reynolds stress tensor

$$v'_i = \langle v'_i v'_i \rangle^{1/2} ,$$

which permits taking into account the turbulence anisotropy [13, 14].

5. Simulation of large vortices or direct numerical simulation of turbulent flows, which permits calculating instantaneous parameters of the flow of filtered or complete Navier–Stokes equations [11, 15]. The mean of the flow is obtained as a result of the time-averaging, and the fluctuation parameters — as the difference between the instantaneous and mean values. The realization of the approach requires large computational costs. However, it makes it possible

to do without introducing empirical corrections and calculate the coherent vortex structures that control the impurity dispersion [6].

Modeling of the Dispersed Phase. The equations describing the translational motion of a spherical probe particle are of the form

$$\frac{d\mathbf{r}_p}{dt} = \mathbf{v}_p, \quad (1)$$

$$\frac{d\mathbf{v}_p}{dt} = \frac{3C_d\rho}{8\rho_p r_p} |\mathbf{v} - \mathbf{v}_p| (\mathbf{v} - \mathbf{v}_p). \quad (2)$$

To calculate the drag coefficient, the following dependence is usually used:

$$C_d = \frac{24}{\text{Re}_p} f_d(\text{Re}_p).$$

The function f_d takes into account the correction for the particle sluggishness in the Stokes law. The Reynolds number in the relative motion of the particle and the carrier gas is found by the formula

$$\text{Re}_p = \frac{2r_p\rho |\mathbf{v} - \mathbf{v}_p|}{\mu}.$$

The temperature-variation equation characterizing the convective heat exchange between the spherical particle and the carrier gas is written in the form

$$\frac{dT_p}{dt} = \frac{3\alpha}{c_p^m \rho_p r_p} (T - T_p). \quad (3)$$

The heat-transfer coefficient of the particle is expressed in terms of the Nusselt number $\text{Nu}_p = 2r_p\alpha/\lambda$ calculated with the use of the dependence

$$\text{Nu}_p = 2 + 0.459 \text{Re}_p^{0.55} \text{Pr}^{0.33}.$$

Equations (1)–(3) are integrated along the trajectory of an individual particle and require only the initial conditions — coordinates, velocity, and temperature of the particle at $t = 0$.

The carrier-gas velocity and temperature in Eqs. (2) and (3) represent random functions of spatial coordinates and time, and their determination in the general case is a rather complicated problem.

Influence of Turbulence on the Particle Motion. Account of the carrier gas turbulence in the dispersed impurity behavior is taken by using the random fluctuations of the carrier flow velocity in the equation of motion of the particle (2). The carrier-medium velocity is given as the sum of the averaged component $\langle \mathbf{v} \rangle$ and the random quantity \mathbf{v}' . The mean velocity component is considered to be given (calculated beforehand on the basis of one of the above approaches), and the fluctuation component is calculated on the basis of the Monte Carlo method. To this end, the model of the particle interaction with turbulent moles is used [4].

The turbulence field is simulated by a set of spherical vortices, each of which is characterized by some velocity \mathbf{v}_e , size L_e , and lifetime t_e .

In the simplest case, the characteristics of turbulent vortices are assumed to be constant throughout the flow field [16].

In the model of [4], the vortex velocity is considered to be a random parameter and is found from the relation

$$\mathbf{v}_e = \{u_e, v_e, w_e\} = \{R_u u', R_v v', R_w w'\}.$$

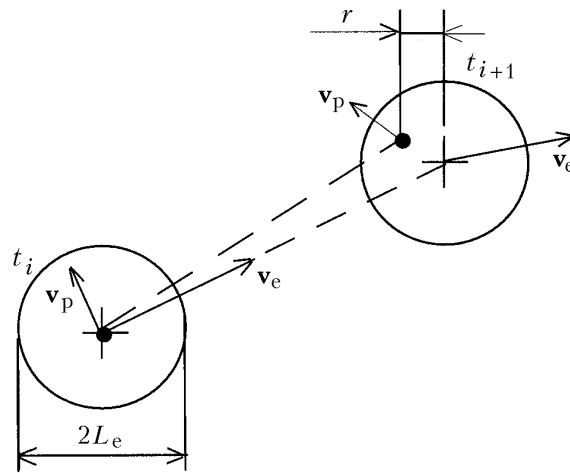


Fig. 2. Particle-turbulent mole interaction, the case where the particle does not leave the initial pulsation mole ($r < L_e$ and $t_{i+1} - t_i < t_e$).

The vortex parameters are determined from the local characteristics of the turbulent flow:

$$L_e = c_\mu^{3/4} \frac{k^{3/2}}{\varepsilon}, \quad t_e = \frac{L_e}{(2k/3)^{1/2}} \quad (c_\mu \sim 0.9).$$

In so doing, it is assumed that during the lifetime of the vortex its velocity and size remain unchanged. Thus, the turbulent mole loses and acquires its individuality stepwise, which, in the final analysis, leads to the appearance of turbulent flow pulsations.

In the model of [17], the vortex lifetime is considered to be a random quantity and is chosen from the Poisson distribution

$$p(t_e) = \frac{1}{t_L} \exp(-t_e/t_L).$$

Interaction of the Particle with Turbulent Moles. Let at some point of the flow a gas mole — a gas volume, whose dimensions are characterized by an integral scale of turbulence — be formed. When moving, the gas mole entrains particles that have gotten into it. The friction between the gas and the particles retards the mole, and the particles are accelerated. The mole retains its pulsation velocity throughout its lifetime (from the moment it was released from one layer of the flow until it mixed with another layer). The mole loses its individuality stepwise.

Suppose that at time t_i a particle having velocity \mathbf{v}_p is in the center of a vortex moving with velocity \mathbf{v}_e (Fig. 2). Taking into account the relative motion of the vortex and the particle at time t_{i+1} , the following three situations are possible: (1) the particle remains within the initial turbulent mole and is moving together with it ($r < L_e$); (2) the particle leaves the initial mole ($r > L_e$); (3) the lifetime of the vortex expires and it loses its individuality ($t_{i+1} - t_i > t_e$), and the particle thereby gets into a new turbulent mole and begins a new process of interaction.

In the case of (1), in accordance with the new position of the particle and the local characteristics of the turbulence, the new values of the characteristic vortex scales (velocity, size, and lifetime) are calculated. In so doing, random numbers R_u , R_v , and R_w are generated at the start of each interaction and subsequently remain unaltered.

In the cases of (2) and (3), the particle gets into a new turbulent mole with different characteristics. The new fluctuation of the carrier flow velocity is determined.

The time in which the particle manages to leave the initial mole is estimated from the linearized equation of motion of the particle:

TABLE 1. Criteria for Generation of a New Fluctuation of the Carrier-Flow Velocity in Different Models

Criterion number	Time criterion t	Space criterion L	Literature source
1	const	const	–
2	$\min\left(\frac{L_e}{\sqrt{2k/3}}, -\tau_p \ln\left(1 - \frac{L_e}{\tau_p \mathbf{v} - \mathbf{v}_p }\right)\right)$	L_e	[14]
3	$\left[\frac{\sqrt{2k}}{2L_e} + \frac{ \mathbf{v} - \mathbf{v}_p }{L_e}\right]^{-1}$	–	[5]
4	$\min\{t_{\max}, t_c\}$	L_e	[10, 19]
5	$\frac{L_e}{\sqrt{2k/3}}$	–	[16]
6	Vortex lifetime is chosen from the Poisson distribution	–	[17]
7	$\min\left(\frac{L_e}{\sqrt{2k/3}}, \frac{L_e}{ \mathbf{v} - \mathbf{v}_p }\right)$	–	[18]

$$t_c = -\tau_p \ln\left(1 - \frac{L_e}{\tau_p |\mathbf{v} - \mathbf{v}_p|}\right).$$

The dynamic relaxation time of the particle is calculated by the relation

$$\tau_p = \frac{8}{3} \frac{\rho}{\rho_p} \frac{r_p}{C_d |\mathbf{v} - \mathbf{v}_p|}.$$

If $L_e > \tau_p |\mathbf{v} - \mathbf{v}_p|$, then the expression for t_c loses meaning. This means that the particle does not leave the given vortex and remains in as long as it exists. Hence, as a time criterion for the generation of a new fluctuation, the minimum of the vortex lifetime t_e and the time in which the particle passes through the vortex t_c is used, namely

$$t = \begin{cases} \min(t_e, t_c), & \text{if } L_e > \tau_p |\mathbf{v} - \mathbf{v}_p|, \\ t_e, & \text{if } L_e \leq \tau_p |\mathbf{v} - \mathbf{v}_p|. \end{cases}$$

The model of [12] assumes that the particle does not leave the initial mole, which creates an overestimated dispersion of particles. Account of the relative motion of the particle and vortex leads to a better agreement between theoretical and experimental data [6, 11].

Comparison of Different Models. The time and space criteria for the generation of a random velocity component of the medium carrier for different models are given in Table 1.

In the model of [16], the integration step is assumed to be equal to t_e . Such an approach means that as long as it lives the mole interacts with the same particles (particles do not enter the model and do not leave it). This holds only for averaged-motion equilibrium turbulent flows. If the mean phase velocities differ, the particles pierce the mole and, in so doing, because of their interaction, their velocities are not equal at the entrance to the mole and at the exit from it. As a result, the particles either carry away with them part of the mole's momentum or transfer to the mole part of their momentum.

Extension of the model of [16] to more complicated cases requires taking into account the relative motion of the particle and the mole.

In the model of [20], the integration step is chosen so that the particle crosses no more than one cell of the computational mesh. Such an approach, however, is computational rather than reflecting actual processes. The ideas proposed in [4] proved to be more advanced, and subsequently they were used many times to calculate various flows [8–11, 15, 21].

In the model of [4], two time scales are introduced. As a time criterion, the minimum from the vortex lifetime and the time in which the particle passes through the vortex is used, and the space criterion is the integral scale of turbulence.

In the gravitational field, solid particles can scatter more intensively than liquid particles [6, 19]. In the model of [19], the maximum particle–turbulent-mole interaction time t_{\max} , which is independent of the solid–liquid-particle interaction time t_f , is introduced. The time t_{\max} is determined on the basis of experimental data by the Lagrangian and Euler scales of turbulence related by the relation

$$t_L = \beta t_E, \quad \beta = \frac{v' t_e}{L_e}.$$

The criterion for the generation of a new fluctuation of the gas-phase velocity is of the following form [19]:

$$t = \begin{cases} \min(t_{\max}, t_c), & \text{if } 2L_e > \tau_p |\mathbf{v} - \mathbf{v}_p|, \\ t_f = 2t_L, & \text{if } 2L_e \leq \tau_p |\mathbf{v} - \mathbf{v}_p|. \end{cases}$$

The factor 2 takes into account the correction for experimental data. The model of [4] assumes that $t_{\max} = t_f = t_e$.

To take into account the turbulence anisotropy, the vortex lifetime is given in the form of the tensor [6, 13]

$$t_{eij} \sim \left(\frac{k^2}{v_i^2 v_j^2} \right)^{1/4} \frac{k}{\varepsilon}.$$

Such an approach calls for turbulence models for second moments. The model of [13] leads to an increase in computational costs with no marked increase in the accuracy of calculations [6].

In many models, the particle velocity is given as a superposition of the convective and diffusion components [3]. The first component is calculated on the basis of the deterministic approach, and the second one is assumed to be proportional to the concentration gradient of the dispersed phase. The impurity concentration is calculated from the diffusion equation. To the thus-found particle shift the random value chosen from the normal distribution in accordance with the turbulent diffusion coefficient of impurity is added. However, because of the difficulty of calculating effective dispersed phase transfer coefficients, such an approach has not found wide use.

Estimates show that for internal and jet flows the account of the criterion t_{\max} introduced in [10, 19] has a weak effect on the impurity scattering, since the criterion for the generation of a new fluctuation of the gas-phase velocity is largely determined by the time t_c . This conclusion is also confirmed by the calculations by the particle dispersion in the mass force field [14].

The results of the calculations indicate that the realization of the stochastic model proves to be insensitive to the choice of the criterion for the generation of a new fluctuation of the carrier flow velocity (except for criterion 1, which is known to be unrealistic). The conclusion drawn is corroborated by the results of [5], where criteria 2–4 are compared.

Unlike the model of [4] in which the velocity fluctuation being calculated is assumed to be constant (is frozen) inside the vortex during its lifetime, the model realized in the present paper considers that the particle is always under the action of the local turbulence at a point connected with its position. For this purpose, the fluctuations obtained at the start of the particle–vortex interaction are multiplied by the local turbulence intensity. Possibly, such an approach will permit taking into account the turbulence inhomogeneity as well as the compression and tension of turbulent vortices.

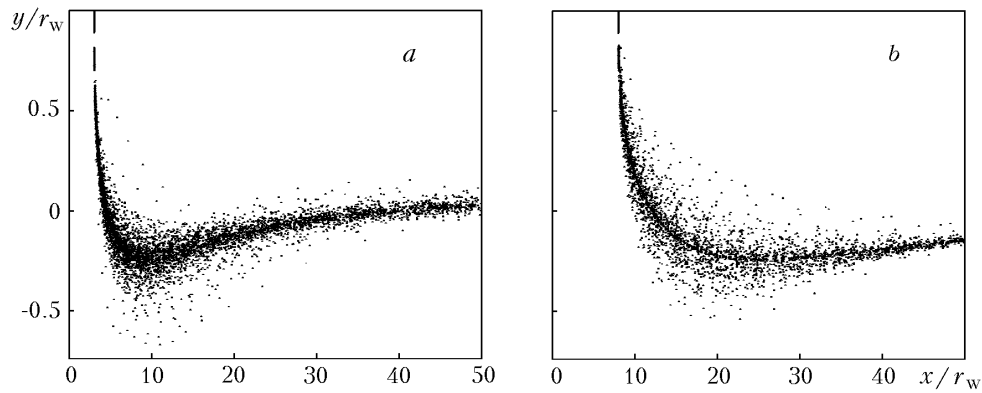


Fig. 3. Realization of random trajectories of particles of $r_p = 10 \mu\text{m}$ in the channel with penetrable walls at $v_w = 5 \text{ m/sec}$; a and b correspond to different coordinates of the point of particle injection from the mass-supplying surface of the channel.

Passage to Mean Parameters. This process is realized by averaging over a large number of particles. The coordinates and velocity averaged over an ensemble of realizations are found by the formulas

$$D_x(t) = \left[\frac{1}{N_p} \sum_{i=1}^{N_p} [x_{pi}(t) - x_{pi}(t_0)] \right]^{1/2}, \quad D_u(x) = \left[\frac{1}{N_p} \sum_{i=1}^{N_p} [u_{pi}(x) - u_{pi}(x_0)] \right]^{1/2}.$$

Here $x_{pi}(t)$ and $x_{pi}(t_0)$ are the particle position at times t and t_0 ; $u_{pi}(x)$ and $u_{pi}(x_0)$ are the velocity of the particle that has crossed the coordinate x_i and the initial velocity of the particle, respectively.

Using the stochastic modeling data, it is deemed to be possible to calculate the second moments of the velocity and temperature pulsations of the carrier and dispersed phases. In particular, the second moments are calculated by the formula

$$\langle v_i' v_{pi}' \rangle = \frac{1}{\Delta t_E N_p} \sum_{m=1}^{N_t} \sum_{n=1}^{N_p} [(v_i - \langle v_i \rangle) (v_{pi} - \langle v_{pi} \rangle)] \Delta t_L.$$

Here $\Delta t_E = N_t \Delta t_L$. Summation over m is done for time averaging over the Euler time step, and summation over n — for averaging over the ensemble of particles in each mesh cell.

Results of the Calculations. To describe the impurity motion and scattering on the basis of the stochastic model, it is necessary to calculate the trajectories of a large number of probe particles. To solve the Cauchy problem, we used the fourth-order Runge–Kutta method and methods that permit resolving in the solution rapidly and slowly decaying components. To supply carrier-gas parameters at points lying in the particle trajectory, we used the bilinear interpolation method. The integration step along each trajectory was limited to the time and space turbulence scales. In the calculations, from 1000 to 10,000 trajectories of probe particles depending on their size were modeled. On average, to calculate the trajectory of a probe particle on the basis of the stochastic model, 25 times more computer time is needed than for the deterministic approach. A decrease in the particle size led to an increase in the number of realizations required for obtaining a statistically reliable averaged pattern of the impurity motion because of the increase in the contribution of the particle interaction with vortices of smaller and smaller sizes.

As examples of using the stochastic model, Figures 3–6 present the results of the calculations of the motion and scattering of aluminum oxide particles ($r_p = 5\text{--}50 \mu\text{m}$) in a channel with penetrable walls (particles are blown in from the side surface of the channel) and in a submerged heated air jet (at longitudinal and transverse injection of particles from the nozzle exit section). To calculate the medium flow field of the carrier phase, the two-parametric dissipative turbulence model [8, 21] was used. For the channel, the injection velocity is assumed to be constant

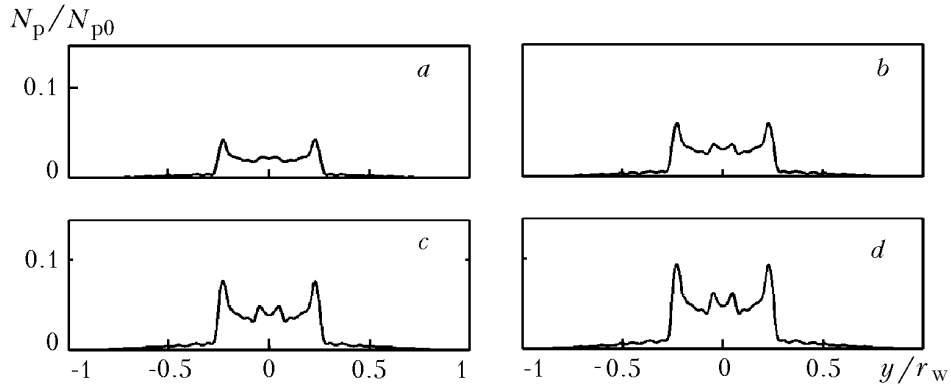


Fig. 4. Distribution of particles of $r_p = 10 \mu\text{m}$ over the channel cross section at $x/r_w = 20$ (a), 30 (b), 40 (c), and 50 (d).

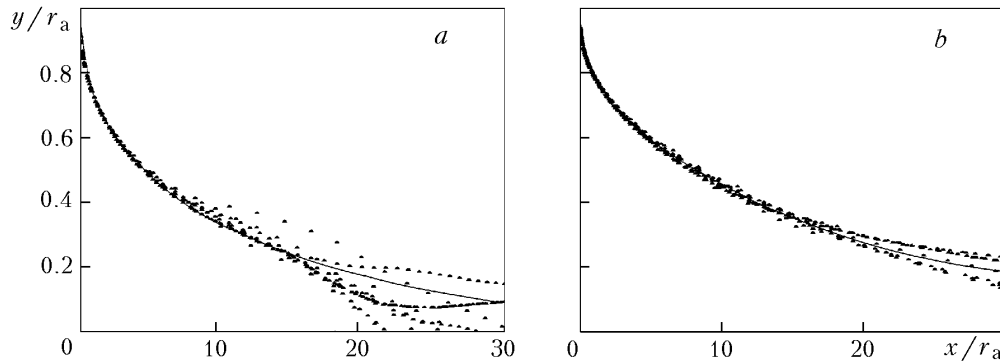


Fig. 5. Realization of random trajectories of particles of $r_p = 10 \mu\text{m}$ (a) and $r_p = 50 \mu\text{m}$ in a submerged jet in the case of transverse injection of particles onto the nozzle exit section for $y_p/r_a = 1.0$ and $v_{p,a} = 2.7 \text{ m/sec}$.

along its generatrix and equal to $v_w = 5 \text{ m/sec}$; for particles $u_{p,w} = 0$ and $v_{p,w} = v_w$. For the jet, the initial parameters of the gas and dispersed phases are as follows: $r_a = 5 \text{ mm}$, $u_a = 97.5 \text{ m/sec}$, $T_a = 400 \text{ K}$, $T_\infty = 300 \text{ K}$, $k_a/u_a^2 = 0.0004$, $\varepsilon_a r_a/u_a^3 = 0.0004$, $u_{p,a} = 0\text{--}97.5 \text{ m/sec}$, $v_{p,a} = 0\text{--}5 \text{ m/sec}$, and $T_{p,a} = 300 \text{ K}$. Solid lines in the figures correspond to the results obtained by averaging over an ensemble of particles; dots show the realization of random trajectories of particles.

The turbulence-field inhomogeneity of the carrier phase in the presence of a considerable kinetic energy minimum in the near-axis region of the flow [8, 21] (in both the injection channel and the submerged jet) for particles of small fractions ($r_p \sim 5\text{--}10 \mu\text{m}$) leads to the appearance of turbulent migration of a particle (turbophoresis force) towards a decrease in the pulsation energy of the gas (Fig. 3). In the penetrable wall channel, there is an increase in the impurity concentration in the vicinity of the envelope of particle trajectories (Fig. 4). Small particles moving in the jet migrate towards the jet axis (Fig. 5a).

For particles of large fractions ($r_p \sim 50 \mu\text{m}$), velocity pulsations have no appreciable effect on the impurity motion throughout the area of flow development because of the sluggishness of such particles (Figs. 5b and 6). However, in this case, too, there is a small migration of particles towards a decrease in the gas pulsation energy.

In general, the influence of the sluggishness of a particle on its scattering is inconclusive, since particles of different masses execute motion in different regions with a different turbulence intensity. The influence of turbulent velocity pulsations on the particle motion is manifest when the particle gets into the turbulent region of the flow (as soon as it crosses the kernel of constant conditions). For example, in the case of transverse injection from the nozzle exit section (Fig. 5), the particle crosses the kernel of constant conditions of the initial area at $y/r_a = 0.6$ and gets into the mixing zone with a level of turbulent pulsations of the order of 6–18%. In the case of longitudinal injection with the initial zero velocity $u_{p,a} = 0 \text{ m/sec}$ and the velocity equal to the flow velocity $u_{p,a} = 97.5 \text{ m/sec}$, the trajectories deflect towards the jet axis (Fig. 6).

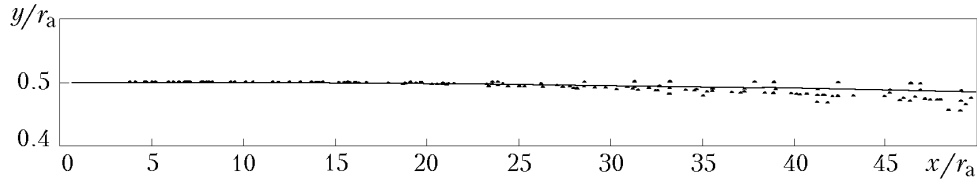


Fig. 6. Realization of random trajectories of particles of $r_p = 50 \mu\text{m}$ in a submerged jet in the case of their longitudinal injection onto the nozzle exit section for $y_p/r_a = 0.5$ and $u_{p,a} = 97.5 \text{ m/sec}$.

A nonmonotonic change in the kinetic energy of turbulent pulsations along the axial coordinate leads to a nonmonotonic change in the degree of particle involvement in the pulsation gas flow, which is determined by the relation between the dynamic relaxation time of the particle and the characteristic time scale of the turbulence.

The calculations performed for light particles with a density of the order of 100ρ show that the stochastic model yields overestimated values of the rms displacement of particles. This is likely to be due to the necessity of taking into account, in the equation of particle motion, the force factors associated with nonstationary effects, in particular, the Basset forces and virtual mass.

CONCLUSIONS

The simulation of the processes of turbulent momentum and heat transfer in low-concentration gas-dispersed systems from the point of view of the stochastic variant of the discrete-trajectory approach shows that carrier-flow velocity pulsations strongly influence the motion and scattering of a dispersed impurity, and the model constructed leads to satisfactory results consistent with the data of numerical and physical experiments.

The application of models taking into account the impurity dispersion in a turbulent flow makes it possible, in particular, to explain some anomalous phenomena observed in experiments, e.g., such as particle pinching in the near-axis region of the flow, as well as escape of particles from the jet as they are longitudinally blown onto the nozzle exit section.

Further development of the stochastic approach is associated with the refusal to model the probability distribution of fluctuating parameters of the carrier flow by the normal distribution. It should be noted that to simulate the carrier-gas flow it is necessary to use approaches that permit obtaining more detailed information on the solution rather than Reynolds-averaged Navier–Stokes equations, e.g., the method of simulating large vortices or direct numerical simulation.

NOTATION

c , specific heat, $J/(kg \cdot K)$; c_μ , constant of the two-parametric model of turbulence; C_d , drag coefficient of the particle; D , dispersion; f_d , drag function; k , kinetic energy of turbulent pulsations, m^2/sec^2 ; L , characteristic linear scale, m ; N_p , number of particles in a cell; N_t , number of Lagrangian time steps in each Euler step; Nu , Nusselt number; p , probability density; Pr , Prandtl number; r , radius, m ; \mathbf{r} , radius vector, m ; R_u, R_v, R_w , random numbers chosen from the normal probability distribution with a zero mathematical expectation and unit dispersion; Re , Reynolds number; t , time, sec ; T , temperature, K ; u, v, w , velocity component, m/sec ; \mathbf{v} , velocity vector, m/sec ; α , heat-transfer coefficient; β , proportionality coefficient; ε , dissipation rate of turbulent energy, m^2/sec^3 ; λ , heat conductivity, $W/(m \cdot K)$; μ , dynamic viscosity, $kg/(m \cdot sec)$; ρ , density, kg/m^3 ; τ_p , dynamic relaxation time, sec ; ω , frequency, $1/sec$; $\langle \dots \rangle$, time averaging. Subscripts: a , nozzle exit section; c , on the time the particle passes through the turbulent mole; d , on the characteristics of the particle drag; e , turbulent vortex; E , on Euler characteristics of turbulence; f , on the interaction time of a solid and a liquid particle; i, j , tensor indices; L , on Lagrangian characteristics of turbulence; m, n , summation indices; max , maximum; p , particle; x , on spatial characteristics; u , on velocity characteristics; w , wall; 0 , initial instant of time; inf , infinity; $'$, pulsations of parameters.

REFERENCES

1. É. P. Volkov, L. I. Zaichik, and V. A. Pershukov, *Modeling of Solid Fuel Combustion* [in Russian], Nauka, Moscow (1984).
2. A. A. Shraiber, L. B. Gavin, V. A. Naumov, and V. P. Yatsenko, *Turbulent Flows of Gas Suspension* [in Russian], Naukova Dumka, Kiev (1987).
3. C. T. Crowe, T. R. Troutt, and J. H. Chung, Numerical models for two-phase turbulent flows, *Ann. Rev. Fluid Mech.*, **28**, 11–43 (1996).
4. A. D. Gosman and E. Ioannides, Aspects of computer simulation of liquid-fueled combustors, *AIAA Paper*, No. 81-0323.
5. N. Cesco, L. Dumas, T. Pevergne, and Y. Fabignon, Stochastic models to the investigation of slag accumulation in a large solid rocket motors, *AIAA Paper*, No. 97-2785.
6. D. Lakehal, On the modelling of multiphase turbulent flows for environmental and hydrodynamic applications, *Int. J. Multiphase Flow*, **28**, 823–863 (2002).
7. G. F. Gorshkov, Propagation of co-current nonisothermal jets of gas and plasma of variable composition, in: *Dynamics of Inhomogeneous and Compressed Media* [in Russian], LGU, Leningrad (1984), pp. 164–175.
8. K. N. Volkov and G. F. Gorshkov, Modeling of the processes of turbulent momentum and heat transfer in non-isothermal dispersion jets, in: *Proc. IV Minsk Int. Forum "Heat and Mass Transfer–MIF- 2000"* [in Russian], Vol. 6, 22–26 May 2000, Minsk (2000), pp. 203–212.
9. K. N. Volkov and G. F. Gorshkov, Heat transfer of disperse impurity particles in turbulent gas and plasma jets, in: *Proc. 3rd Russ. Nat. Conf. on Heat Transfer* [in Russian], Vol. 5, 22–25 October 2002, Moscow (2002), pp. 187–190.
10. D. I. Graham and P. W. James, Turbulent dispersion of particles using eddy interaction models, *Int. J. Multiphase Flow*, **22**, No. 1, 157–175 (1996).
11. E. A. Matida, K. Nishino, and K. Torii, Statistical simulation of particle deposition on the wall from turbulent dispersed pipe flow, *Int. J. Heat Fluid Flow*, **21**, 389–402 (2000).
12. Y. Wang and P. W. James, On the effect of anisotropy on the turbulent dispersion and deposition of small particles, *Int. J. Multiphase Flow*, **25**, 551–558 (1999).
13. D. Burry and G. Bergeles, Dispersion of particles in anisotropic turbulent flows, *Int. J. Multiphase Flow*, **19**, 651–664 (1993).
14. X.-Q. Chen, Heavy particle dispersion in inhomogeneous, anisotropic turbulent flows, *Int. J. Multiphase Flow*, **26**, 635–661 (2000).
15. K. Volkov, Large eddy simulation of non-isothermal turbulent gas-particle jets, in: B. J. Bath (ed.), *Computational Fluid and Solid Mechanics*, Elsevier (2003), pp. 42–45.
16. J. K. Dukowicz, A particle-fluid numerical model for liquid sprays, *J. Comput. Phys.*, **35**, No. 2, 229–253 (1980).
17. M. Sommerfeld and G. Zivkovic, Recent advances in the numerical simulation of pneumatic conveying through systems, in: *Computational Methods in Applied Sciences*, Elsevier (1992), pp. 201–212.
18. J. F. Chauvot, L. Dumas, and K. Schmeisser, Modelling of Alumina Slag Formation in Solid Rocket Motors, *AIAA Paper*, No. 95-2728.
19. D. I. Graham, Improved eddy interaction models with random length and times scales, *Int. J. Multiphase Flow*, **24**, No. 2, 335–345 (1998).
20. J. S. Sabnis, S.-K. Choi, R. C. Buggeln, and H. J. Gibeling, Computation of Two-Phase Shear-Layer Flow Using an Eulerian–Lagrangian Analysis, *AIAA Paper*, No. 88-3202.
21. K. N. Volkov and V. N. Emel'yanov, A stochastic model condensed particle motion in a channel with penetrable walls, *Mat. Modelir.*, **11**, No. 3, 105–111 (1999).